

# Acoustic Velocities and Pillar Monitoring On the 4850 Level of the Sanford Underground Research Facility

Roggenthen, W.M. and Berry, K.M.

*Dept. of Geology and Geological Engineering, South Dakota School of Mines and Technology, Rapid City, SD USA*

Copyright 2016 ARMA, American Rock Mechanics Association

This paper was prepared for presentation at the 50<sup>th</sup> US Rock Mechanics / Geomechanics Symposium held in Houston, Texas, USA, 26-29 June 2016. This paper was selected for presentation at the symposium by an ARMA Technical Program Committee based on a technical and critical review of the paper by a minimum of two technical reviewers. The material, as presented, does not necessarily reflect any position of ARMA, its officers, or members. Electronic reproduction, distribution, or storage of any part of this paper for commercial purposes without the written consent of ARMA is prohibited. Permission to reproduce in print is restricted to an abstract of not more than 200 words; illustrations may not be copied. The abstract must contain conspicuous acknowledgement of where and by whom the paper was presented.

The Sanford Underground Research Facility (SURF) has repurposed older workings of a long-lived gold mine to host scientific experiments. The present laboratories are developed primarily in Precambrian-age amphibolite host rock, but Tertiary-age rhyolite intrusives are also present. A portion of the pillar in the vicinity of the new physics laboratories on the 4850 level (1.5 km below the surface) was chosen for examination using seismic tomography to evaluate the degree and location of potential pillar degradation. Geophones and sources were placed on opposite sides of a pillar formed by the intersection of two drifts, and an acoustic wave was passed between them to produce multiple paths along which the P-wave velocities were calculated. The resulting tomographic velocity map of the pillar adjacent to the intersection shows a well-developed pattern of decreasing velocities toward the acute end of the triangle due to a decreasing pillar cross-section. Higher seismic velocities are associated with areas where the stresses are greater but where the rock has not failed, such as adjacent to well-maintained drifts.

## 1. Introduction

The Sanford Underground Research Facility (SURF) is being developed as an underground scientific laboratory in a former gold mine in northwestern South Dakota, USA (Heise, 2015; Lesko et al., 2011). The underground workings are extensive and have a history that extends over 125 years. The facility is a host for a number of existing and planned physics experiments that require shielding from cosmic radiation along with a lesser number of geological, geomechanical, and biological experiments. Although it is still indeterminate, a design life of 30 years is not unreasonable for this type of facility. Given the age of much of the underground infrastructure and the expected long operational life of the facilities, it is important to have monitoring programs that can assess the condition of rock making up the underground infrastructure. Such programs will allow evaluation of the necessity for mitigation of degradation of rock conditions. The purpose of the present study was to image the conditions of the rock in a pillar at the 4850 Level of the facility (1.5 km below the surface) near a critical part of the underground infrastructure.

The geology of the mine and of the rocks that constitute SURF was studied extensively during the 125 years

when it was an active gold mine. Caddy, et al., 1991, and Bachman and Caddy, 1990, provide the most recent summary of the geologic environment in terms of the overall geology. More recent studies of the geotechnical characteristics of the rock in the vicinity of the physics laboratories on the 4850 Level were performed as part of the scoping for early versions of the laboratories (Hladysz et al, 2011). Geotechnical work is continuing as the experiment areas are expanded and developed.

Figure 1 shows the drifts and workings on the 4850 Level where this investigation was conducted. The circled area encloses the Davis Campus, the site of many of the physics experiments. The rocks in the circled area are primarily Precambrian amphibolites with varying amounts of Tertiary-age rhyolite intrusive rocks. From an operational standpoint, the drift intersection immediately adjacent to the Yates Shaft station is important to the critical infrastructure of the area. The span of the intersection is relatively wide, is adjacent to many of the current laboratory areas, and is a major staging area for personnel and equipment at the Yates Shaft Station. However, the rock is undergoing degradation in the triangular area where the east and west drifts meet near the Yates Shaft at the intersection of four major drifts (Fig. 1). The point of the triangle shown in Figure 1 has undergone obvious fracturing and

general loosening of the otherwise excellent geomechanically stable rock making up this

operated a seismic array to monitor active seismicity near the 7100 Level (2.2 km below the surface) that was associated with mining activities. Friedel et al., 1996, performed a seismic tomography study in approximately the same area to understand the stress distribution in the drifts and mined areas.

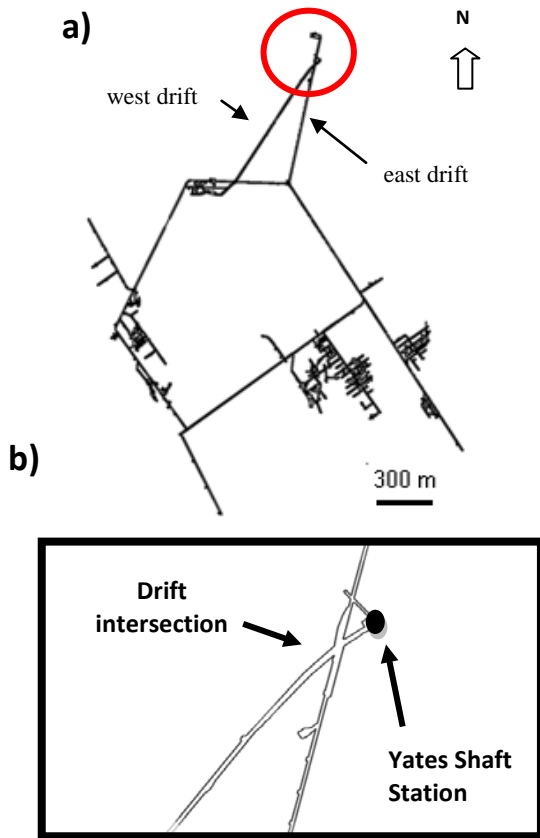


Fig. 1. a) Generalized map of the 4850 and b) the location of the triangle studied, which is south of the major intersection of the four drifts.

portion of the underground. The rhyolite is a somewhat complicating factor in that its geomechanical properties are substantially different from those of the amphibolites (Hladysz, 2011), but this rock type only occurs to the south further away from the triangle point. Although the original laboratories were developed in the amphibolite, experiment areas are being constructed in the phyllites of the upper part of the Poorman Fm., e.g. Hladysz et al., 2011 and Caddy et al., 1991, illustrate stratigraphic relationships and provide further information regarding rock types.

The goal of the present study was to determine seismic velocity variations that could indicate where the rock strength was compromised. With regard to previous work, a distinction can be made between seismic methods using an active, artificial source and those that rely upon natural or induced seismicity. Previous engineering seismic studies at the SURF location include Filigenzi and Girard, 1995, and Girard et al., 1995, who

In terms of general relationships, studies of the quantitative relationships between sonic velocity and rock strength tend to concentrate on sedimentary rocks with some exceptions due to the issues related to weaker rocks in coal mines, the availability of sonic logs from boreholes, and its importance in hydraulic fracturing (Changdong et al., 2006). Much of the response of sedimentary rocks results from the interaction between pores and rock matrix. In the case of the SURF underground and the Yates unit, only rare porosity due to macrofracturing is present in the crystalline rocks although presumably macrofractures of unknown extent are also present. Therefore, it is important to distinguish between poroelastic effects as might be found in sedimentary rocks as opposed to effects modifying velocities in tight crystalline rocks, such as those that constitute the Yates unit at SURF. Although the theoretical acoustic velocity of a rock can be estimated based on its mineralogy (Simmons, 1975) or its composition (Behn and Kelemen, 2003), other effects can decrease the theoretical velocity. For instance, Sano et al. (1992) demonstrated that the velocity in granite was reduced by the existence of microcracking. Microcracks that were favorably oriented with respect to the applied stresses would close as the stress was applied. Therefore, seismic velocity should increase as stress increases and as the fractures close.

## 2. Methodology and Data

The amphibolite of the Yates unit proved to be especially well-suited to the investigation of the distribution of variations in acoustic wave velocities due to its low attenuation characteristics. The data were acquired by installing a series of geophones along the eastern drift shown in Figure 1 and a large hammer was used as the seismic source on the opposing side of the triangle in the western drift of Figure 1. Using a hammer as a seismic source proved to be effective to distances of at least 100 m. First arrivals could be easily identified at these distances except where the rock quality was compromised toward the tip of the triangle. Identification became more difficult at these locations, although choosing the first arrivals was still possible. The receiver mounting system consisted of geophones mounted on an aluminum plate. The plate was affixed to the rib of the drift with a length of threaded bolt that was secured with epoxy in a 2.5 cm diameter drill hole. This ensured a firm coupling between the geophones and

the rock. The travel times between the hammer source and the geophones were measured using a 24-channel, 24-bit seismograph with a nominal 125 microsecond sampling rate. It is not unusual, however, for some variation to occur in the electronics of the digitizer from the selected sampling interval. Because the travel time is critical for the measurements, special care was taken to determine accurate sampling intervals. Therefore, a test area was identified on the surface consisting of a 30 m section of railroad track that was constructed on low-velocity surficial sediments. This assured that the fastest travel path was through the rail. The velocity of the track steel was determined independently using a Pundit™ ultrasonic pulse velocity (UPV) test instrument that was calibrated to NIST standards. The travel time corrections were determined by measuring the rail velocity over the length of the test rail with the seismograph used in this study. These corrections accounting for the variation in sample rates were applied to all of the seismic data subsequent to the data calibration.

The layout of one set of source-receiver pairs is shown in Figure 2. After recording the signal from the source-receiver stations shown, the hammer was moved to the next source station and the process repeated. Figure 3 shows all ray paths used in the analysis of the velocity distribution in the 4850 Level triangle. These paths cover the entire end of the triangle except for the extreme northern end of the triangle where the rock was not of sufficient quality to allow installation of either geophones or use as a source location.

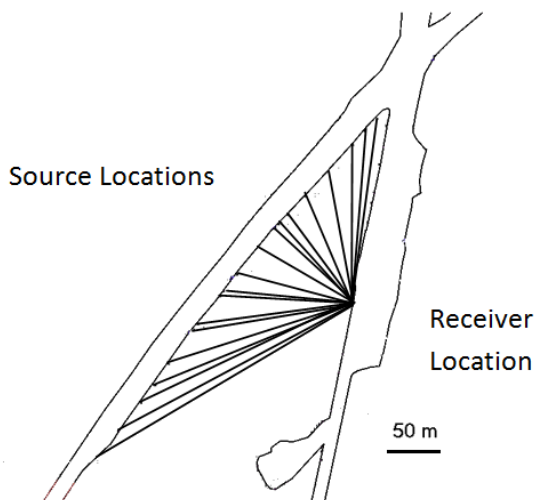


Fig. 2. Example of a receiver location receiving information from multiple sources. This yielded many source-receiver pairs for velocity analysis.

The arrival times from the source-receiver pairs were analyzed using the tomographic software package

GeotomCG™ (Jackson and Tweeton, 1996; Jackson et al., 1995). The resulting distribution of interpreted P-wave velocities are shown in Figure 4 with higher velocities shown as red colors and slower velocities shown as blue. Roggenthen and Koch, 2013, measured sonic velocities of core from this area, and the values found in the tomographic work are consistent with those from this study although the core measurements were not performed under pressure and the effects of larger-scale fractures would also introduce differences. The velocities derived from core data show that the amphibolite has consistently higher velocities than the rhyolite. The current tomographic investigation did not include any of the phyllites on this level that occur to the south where newer excavations are planned.

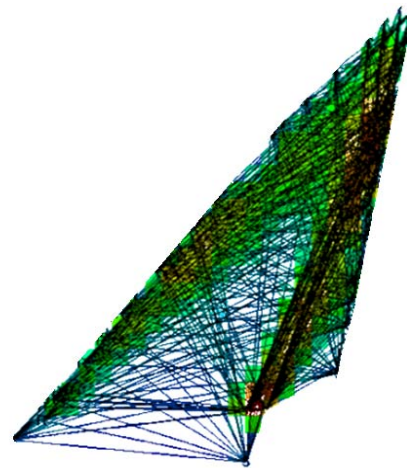


Fig. 3. Source-receiver pairs used in the study.

### 3. Discussion

The pattern of interpreted velocities in Figure 4 is well-defined. In general, low velocities (blue) tend to occur near the end (tip) of the triangle, whereas higher velocities occur away from the end of the triangle where the pillar is thicker. A line drawing of the velocity domains recognized is included as Figure 5. These variations are consistent with expected increases in stress and degradation, which depend upon the stresses and strains acting on the pillar. At lower differential stresses the major effect of increasing confining pressure is crack closure, which probably includes both micro- and macro-fractures. This portion of the diagram is dominated by increased seismic velocities. However, as differential stress increases the dilatancy transitional field, shown diagrammatically in Figure 6, is entered, which leads to decreasing seismic velocities as cracking and fracturing begins to open voids in the rock mass. This appears to be the case toward the tip of the pillar triangle to the north in Figure 1 due to the stresses from the drift intersections to the north along with the thin pillar cross section (Zone B). It should be noted, however, that even though the zone toward the tip of the

triangle shows substantially lower velocities than in the pillar to the south, a core of higher velocity material is still present in the center of the low velocity material (Zone A). This suggests that the center of this zone is still functioning to provide support this portion of the pillar.

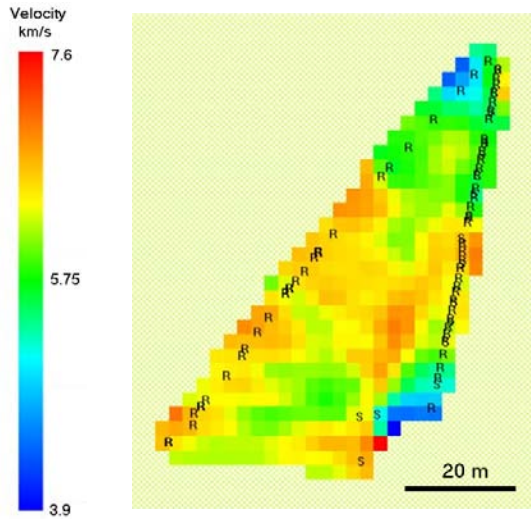


Fig. 4. Interpreted velocities from the pillar on the 4850 Level defined by the west and east drifts.

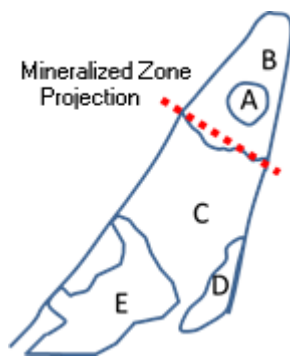


Fig. 5. Velocity domains identified in the velocity structure. Zone A is a higher velocity core within a generally lower velocity area at the tip of the triangle (Zone B). Zone C shows relatively homogeneous higher velocities with a possibility of higher velocities adjacent to the west drift. Zone D has smaller velocities that perhaps are associated with a wider drift along the east side of the pillar. The lower velocities of Zone E may be due to rhyolites within the pillar that are exposed in the west drift in this area. The dashed line is a projection of a mineralized zone exposed in the west drift.

The change from the higher velocities characteristic of the rock in the thicker pillar sections to those with lower seismic velocities toward the tip occurs sharply (Fig. 4; Fig. 5). The change in velocities appears to coincide

with the presence of the thin mineralized zone. The zone is shown in Figure 7 and its orientation of S35°E 54°S was measured where this feature is exposed on the west side of the west drift. Its projection into the pillar is shown in Figure 5. The high concentration of anhydrite in the mineralized zone (Table 1) is consistent with Tertiary-age mineralization. Uzunlar, 1993, determined that anhydrite formed during the early stage mineralization in these systems at the 5900 Level (1800 m below the surface) and below.

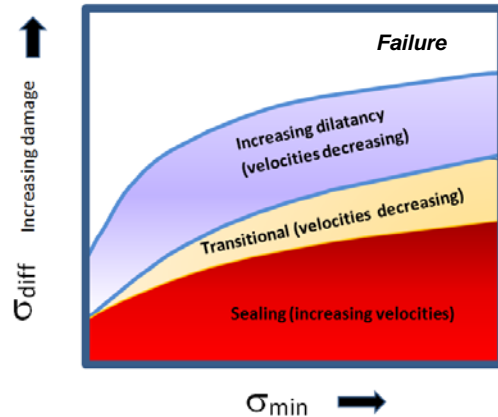


Fig. 6. Schematic relationship between compaction and the development of dilatancy as a function of stress (modified from Popp and Salzer, 2007).

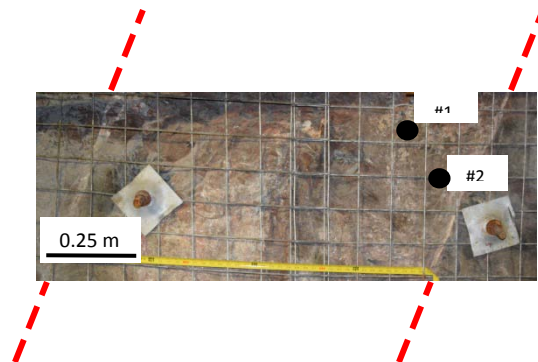


Fig. 7. Mineralized zone marking the transition between lower velocities in the pillar from the higher velocities to the south. The darker areas to the left and right sides of the photograph are amphibolite country rock of the Yates unit. Channel samples taken from the area that is lighter in color sample the mineralized zone and the mineralogical mode for each of the samples is shown in Table 1. The amphibolite sample in Table 1 is shown for comparison and was taken from the country rock in the lower left hand side of the photograph.

The higher velocities along the west drift in Figure 5 (Zone C) are consistent with expected higher stresses resulting from the presence of the drift which transfers stress into the adjacent rock. In comparison, the lower velocities derived for the eastern side of the pillar (Zone

D) may result from a wider drift dimension on the eastern side (Fig. 1) that would lead to the development of zones of lower velocity due to the rock loosening. However, calculation artifacts are possible, and these interpretations should be used with care. The lower velocities of the rhyolites appear to have been imaged to an extent as well (Zone E). The rhyolite crops out in the west drift on the lower left portion of the diagram in Figure 1. Measurement of rock velocities from core shows that the rhyolites typically have velocities substantially lower than the amphibolites (Roggenthen and Koch, 2013).

Table 1. Mineralogical modes of mineralized zone from XRD analysis. MZ-1 and MZ-2 refer to channel samples shown in Fig. 7, and NM-1 is from the non-mineralized Yates amphibolite.

| Mineral (XRD) | MZ-1              | MZ-2              | NM-1        |
|---------------|-------------------|-------------------|-------------|
|               | channel sample #1 | channel sample #2 | amphibolite |
| Feldspar      | 17.9              | 34.5              | 57.5        |
| Anhydrite     | 62.0              | 37.5              |             |
| Biotite       | 1.3               | 0.2               | 0.8         |
| Calcite       | 2.9               |                   |             |
| Chlorite      |                   |                   | 1.6         |
| Hornblende    | 1.6               |                   | 32.2        |
| Pyrite        | 14.2              | 27.7              |             |
| Quartz        |                   |                   | 7.8         |

#### 4. Conclusions

Seismic tomography successfully imaged the condition of the rock in a pillar whose cross-sectional area decreased as a critical infrastructure intersection was approached. The boundary between rock that was degrading near the major intersection near the Yates Shaft is marked by a Tertiary-age mineralized zone. This method can be useful in planning for mitigation of the effects of the increased fracturing in the vicinity of critical infrastructure in the laboratory. Comparison of these results with future investigations should allow quantification of the amount and progress of the degradation as a function of time. The ability to image the presence and approximate locations of the rhyolites may also be useful in those areas of the underground with significant amounts of rhyolite present.

#### 5. Acknowledgements

The assistance of students from the South Dakota School of Mines and Technology including Melissa Heron, Jason Van Beek, and Steve Metzger was appreciated. SURF personnel facilitated the logistics, and Michael Oates was especially helpful in preparation of the

geophone receiver stations. Access to the site was accommodated as part of the geotechnical investigations associated with the Deep Underground Science and Engineering Laboratory Preliminary Design. Funding for these activities was provided by the National Science Foundation through Cooperative Agreements PHY0528103, PHY0717003, PHY0938228, PHY0940801 and PHY10599670. Funding for the velocity measurements was provided by NSF CMMI-0727921.

#### References

- 1) Bachman, R.L. and S.W. Caddey, 1990. "The Homestake mine, Lead, South Dakota: An overview", in *Metallogeny of Gold in the Black Hills*, South Dakota, eds. C. J. Paterson and A.L. Lisenbee, Guidebook Prepared for Soc. Econ. Geol. Field Conf. - 5-9 September, 1990, 89-94. Behn, M. D., and P. B. Kelemen, 2003. Relationship between seismic P-wave velocity and the composition of anhydrous igneous and meta-igneous rocks, *Geochem Geophys Geosyst*, 4: 57p.
- 2) Caddey, S. W., Bachman, R. L., Campbell, T. J., Reid, R. R., and Otto, R. P., 1991. The Homestake Gold Mine, an Early Proterozoic Iron-Formation-Hosted Gold Deposit, Lawrence County, South Dakota. U. S. Geological Survey Bulletin 1857-J, *Geology and Resources of Gold in the United States*, 67 p.
- 3) Changdong, C., M. D. Zoback, and A. Khaksar, 2006. Empirical relations between rock strength and physical properties in sedimentary rocks, *J Petrol Sci Eng*, 51: 223-237.
- 4) Filigenzi, M.T. and J.M. Girard, 1995. Seismic Studies and Numerical Modeling at the Homestake Mine, Lead, SD, in *Proceedings: Mechanics and Mitigation of Violent Failure in Coal and Hard-rock Mines, Special Pub. 01-95*, U.S. Bureau of Mines, 347-355.
- 5) Friedel, M.J., Scott, D.F., Jackson, M.J., Williams, T.J., and Killen, S.M., 1996. 3-D tomographic imaging of anomalous stress conditions in a deep US gold mine: *J Appl Geophys*, 36: 1-17.
- 6) Girard, J.M., T.J. McMahon, W. Blake, and T.J. Williams, 1995. Installation of PC-based Seismic Monitoring Systems with Examples from the Homestake, Sunshine, and Lucky Friday Mines, in *Proceedings: Mechanics and Mitigation of Violent Failure in Coal and Hard-rock Mines, Special Pub. 01-95*, U.S. Bureau of Mines, 303-312.

- 7) Heise, J., 2015, The Sanford Underground Research Facility at Homestake, arXiv:1503.01112 [physics.ins-det].
- 8) Hladysz, Z.J., Callahan, G.D., Popielak, R., Weinig, W., Randolph-Loar, C., Pariseau, and W.G., Roggenthen, W., 2011. Site investigations and geotechnical assessment for the construction of the deep underground science and engineering laboratory, *T I Min Metall A*, 330: 526-542.
- 9) Jackson, M. J., M. J. Friedel, D. R. Tweeton, D. F. Scott, and T. Williams, 1995. Three-dimensional Imaging of Underground Mine Structures Using Seismic Tomography, *Proceedings of the Symposium on the Application of Geophysics to Engineering and Environmental Problems (SAGEEP95)*, Orlando, FL, Apr. 23-26, 221-230.
- 10) Jackson, M.J., and D.R. Tweeton, 1996. 3DTOM: Three-Dimensional Geophysical Tomography, *USBM RI 9617*,.
- 11) Lesko, K.T., S. Acheson, J. Alonso, P. Bauer, Y. Chan, W. Chinowsky, S. Dangermond, J. Detwiler, S. De Vries, R. DiGennaro, E. Exter, F. Fernandez, E. Freer, M. G. D. Gilchriese, A. Goldschmidt, B. Grammann, W. Griffing, B. Harlan, W. C. Haxton, M. Headley, J., Heise, Z. Hladysz, D. Jacobs, M. Johnson, R. Kadel, R. Kaufman, G. King, R. Lanou, A. Lemut, Z. Ligeti, S. Marks, R. D. Martin, J. Matthesen, B. Matthew, W. Matthews, R. McConnell, W. McElroy, D. Meyer, M., Norris, D. Plate, K. E. Robinson, W. Roggenthen, R. Salve, B. Saylor, J. Scheetz, J. Tarpinian, D. Taylor, D. Vardiman, R. Wheeler, J. Willhite, and J. Yeck. 2011. Deep Underground Science and Engineering Laboratory – Preliminary Design Report. <http://arxiv.org/ftp/arxiv/papers/1108/1108.0959.pdf>.
- 12) Popp, T. and K. Salzer, 2007. HE-D Experiment: Influence of bedding planes (IFG), *Mont Terri Project Technical Report 2007-04*, 71 p.
- 13) Roggenthen, W. M. and C. D. Koch, 2013. Geophysical Logging of DUSEL Core and Geotechnical Applications, *47th US Rock Mechanics / Geomechanics Symposium*, San Francisco, CA, USA, 23-26 June 2013, ARMA 13-493.
- 14) Sano, O., Y. Kudo, and Y. Mizuta, 1992. Experimental determination of elastic constants of Oshima Granite, Barre Granite, and Chelmsford Granite, *J. Geophys. Res.*, 97: 3367-3379.
- 15) Simmons, Gene, T. Todd, and W. S. Baldrige, 1975. Toward a quantitative relationship between elastic properties and cracks in low porosity rocks, *Am J Sci*, 275: 318-345.
- 16) Uzunlar, Nuri, 1993. *Genesis of Tertiary Epithermal-Mesothermal Gold-Silver Deposits in the Lead-Deadwood Dome, Northern Black Hills, South Dakota*, unpub. Ph.D. Dissert., South Dakota School of Mines and Technology, Rapid City, SD.